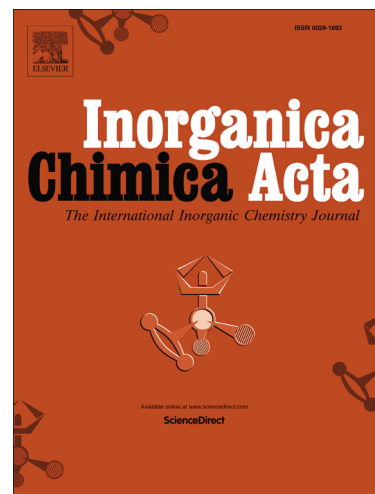


## Journal Pre-proofs

Research paper

Effects of Cu(II) and Zn(II) coordination on the trypanocidal activities of curcuminoid-based ligands

Bianca Almeida da Silva, Paulo Pitasse-Santos, Vitor Sueth-Santiago, Antônio Ricardo Moutinho Monteiro, Roberta Katlen Fusco Marra, Guilherme Pereira Guedes, Ronny Rocha Ribeiro, Marco Edilson Freire de Lima, Debora Decoté-Ricardo, Amanda Porto Neves



PII: S0020-1693(19)31178-8  
DOI: <https://doi.org/10.1016/j.ica.2019.119237>  
Reference: ICA 119237

To appear in: *Inorganica Chimica Acta*

Received Date: 7 August 2019  
Revised Date: 28 October 2019  
Accepted Date: 28 October 2019

Please cite this article as: B.A. da Silva, P. Pitasse-Santos, V. Sueth-Santiago, A.R.M. Monteiro, R.K.F. Marra, G.P. Guedes, R.R. Ribeiro, M.E.F. de Lima, D. Decoté-Ricardo, A.P. Neves, Effects of Cu(II) and Zn(II) coordination on the trypanocidal activities of curcuminoid-based ligands, *Inorganica Chimica Acta* (2019), doi: <https://doi.org/10.1016/j.ica.2019.119237>

This is a PDF file of an article that has undergone enhancements after acceptance, such as the addition of a cover page and metadata, and formatting for readability, but it is not yet the definitive version of record. This version will undergo additional copyediting, typesetting and review before it is published in its final form, but we are providing this version to give early visibility of the article. Please note that, during the production process, errors may be discovered which could affect the content, and all legal disclaimers that apply to the journal pertain.

© 2019 Published by Elsevier B.V.

**Effects of Cu(II) and Zn(II) coordination on the trypanocidal activities of curcuminoid-based ligands**

Bianca Almeida da Silva<sup>1</sup>, Paulo Pitasse-Santos<sup>1</sup>, Vitor Sueth-Santiago<sup>1,2</sup>, Antônio Ricardo Moutinho Monteiro<sup>1</sup>, Roberta Katlen Fusco Marra<sup>1</sup>, Guilherme Pereira Guedes<sup>3</sup>, Ronny Rocha Ribeiro<sup>4</sup>, Marco Edilson Freire de Lima<sup>1</sup>, Debora Decoté-Ricardo<sup>5</sup> and Amanda Porto Neves<sup>1,\*</sup>

<sup>1</sup>Instituto de Química, Universidade Federal Rural do Rio de Janeiro, BR-465 Km 7, CEP: 23890-000, Seropédica, RJ, Brasil. \*E-mail: amandanevess@ufrj.br

<sup>2</sup>Instituto Federal de Educação, Ciência e Tecnologia do Rio de Janeiro, Rua José Augusto Pereira dos Santos, CEP 24425-004, São Gonçalo, RJ, Brasil.

<sup>3</sup>Instituto de Química, Universidade Federal Fluminense, Outeiro de São João Batista, s/n, CEP 24020-150, Niterói, RJ, Brasil.

<sup>4</sup>Departamento de Química, Universidade Federal do Paraná, Cx. Postal 19081, CEP: 81531-980, Curitiba, PR, Brasil.

<sup>5</sup>Departamento de Microbiologia e Imunologia Veterinária, Instituto de Veterinária, Universidade Federal Rural do Rio de Janeiro, BR-465 Km 7, CEP: 23890-000, Seropédica, RJ, Brasil.

## Abstract

Four heteroleptic metal complexes with the general formula  $[M(L1-2)(phen)Cl]$  **1a-b**, **2a-b**, ( $M = Cu(II)$  or  $Zn(II)$ ,  $L =$  curcuminoid ligand and phen = phenanthroline) have been prepared from the reaction of the ligands in the presence of  $Et_3N$  with  $CuCl_2 \cdot 2H_2O$  or  $ZnCl_2$ . Characterization by IR,  $^1H$  NMR and EPR spectroscopies, and X-ray diffraction analysis for **1b** confirmed the proposed structures for the complexes. The curcuminoid ligand coordinates in a deprotonated form as an *O,O* chelate, with phen and chloride completing the coordination sphere of the metal. The cytotoxic effects of ligands (**HL1**, **HL2**, phen) and complexes (**1a-b**, **2a-b**) on the amastigote form of *Trypanosoma cruzi* have been screened. All substances showed significant toxicity. The Zn(II) complexes **1b** ( $IC_{50} = 0.47 \mu M$ ,  $SI = 4.3$ ) and **2b** ( $IC_{50} = 0.40 \mu M$ ,  $SI = 3.8$ ) were the most potent compounds being more toxic and selective against the parasite than the ligands and the copper complexes, thus implying that the coordinating metal is important for the trypanocidal activity of the curcumin-based compounds.

**Keywords:** Curcuminoid, Cu(II) and Zn(II) complexes, *Trypanosoma cruzi*, amastigote, parasite.

## 1. Introduction

Chagas disease (CD), also known as American Trypanosomiasis, is a vector-borne infection transmitted by insects from the *triatominae* subfamily (*Reduviidae*) popularly called kissing bugs [1,2]. The etiological agent of CD, the protozoan *Trypanosoma cruzi* (*T. cruzi*), is endemic to Latin America and according to the World Health Organization (WHO), approximately 6-7 million people worldwide are infected with *Trypanosoma cruzi* [3,4]. Also, 12000 deaths are estimated per year in 21 endemic countries in Latin America [5]. For almost 50 years, the only drug options available for CD have been

benznidazole and nifurtimox, which are effective in the acute phase but less efficient in the chronic phase of the disease. In addition, these drugs are not considered ideal, because of their severe side effects and the possible development of resistance [5,6]. The search for novel chemotherapeutics that show toxic effects selective to parasites without compromising the host organism is the primary paradigm in the search for new antiparasitic drugs. The approach to antiparasitic chemotherapy can be based both on biological targets that are specific to the parasite as well as on those shared by the parasites and their hosts, which have variations that make selectivity possible. In any case, the goal will always be the development of a new drug exerting greater effects on the parasite and fewer deleterious effects on the host [7,8].

Diarylheptanoids comprise a class of natural and synthetic compounds of great interest in medicine, due to their pharmacological profile, such as anticancer, antimicrobial and antifungal activity [9,10]. The most important compound and one of the most popular medicinal herb extracts of this class is curcumin [10,11], which has therapeutic efficacy in skin and autoimmune diseases, as well as proven anti-inflammatory, antioxidant and antiviral activities [12,13,14]. More recently, its effect against *Aedes aegypti* larvae has also been demonstrated [15].

In recent work developed by our group, Sueth-Santiago and co-workers reported the trypanocidal activity of three natural diarylheptanoids isolated from *Curcuma longa* (Zingiberaceae): curcumin, desmethoxycurcumin and bis-desmethoxycurcumin. Curcumin presented an IC<sub>50</sub> value against epimastigotes of *T. cruzi* (Dm28c strain) of 10 µM and is a potential agent for the treatment of *Trypanosoma cruzi* infections [16]. Despite the biological relevance exhibited by curcumin, this compound displays some restrictions on its clinical use, such as low bioavailability and stability, and poor solubility [17-19]. One of the strategies to overcome these drawbacks has been the coordination of

curcumin with metal ions. Such complexes may prevent degradation of curcumin and also enhance its biological activity [20-25]. For instance, complexes containing curcuminoids have been reported for a number of applications, including antiarthritis [26], antimicrobial [27] and, mainly, anticancer [28]. A ruthenium(III) complex containing a curcumin derivative was reported to be cytotoxic against HeLa cells, with an  $IC_{50} = 0.04172$  nM, indicating great anticancer activity [29]. Another important study about oxovanadium(IV) curcumin complexes containing phen and dppz as auxiliary ligands showed the remarkable phototoxicity of curcumin ( $IC_{50} = 8.2$   $\mu$ M) and its respective complexes ( $IC_{50} = 8.1$   $\mu$ M and 3.3  $\mu$ M) against HeLa cells, in which all were less toxic in the dark ( $IC_{50} > 50$   $\mu$ M) [30]. Zinc(II) complexes of curcumin were also shown to induce cell apoptosis [31] and copper(II) complexes of the type  $[Cu(\text{curc-deriv})_2]$  were about 3-5 fold more cytotoxic than the free ligands [32].

Considering that coordination of curcuminoids often results in the improvement of their biological activities, this work aimed at investigating the trypanocidal activity of curcumin (**HL1**) and its carbocyclic analogue (**HL2**) compared with their corresponding Cu(II) and Zn(II) complexes of the type  $[M(\text{L1-2})(\text{phen})Cl]$  (**1a-b**, **2a-b**) (Figure 1). Phenanthroline was chosen as the auxiliary ligand based on previous results that showed greater antibacterial activity of Cu(II) and Zn(II) complexes after coordination with phen [33,34].

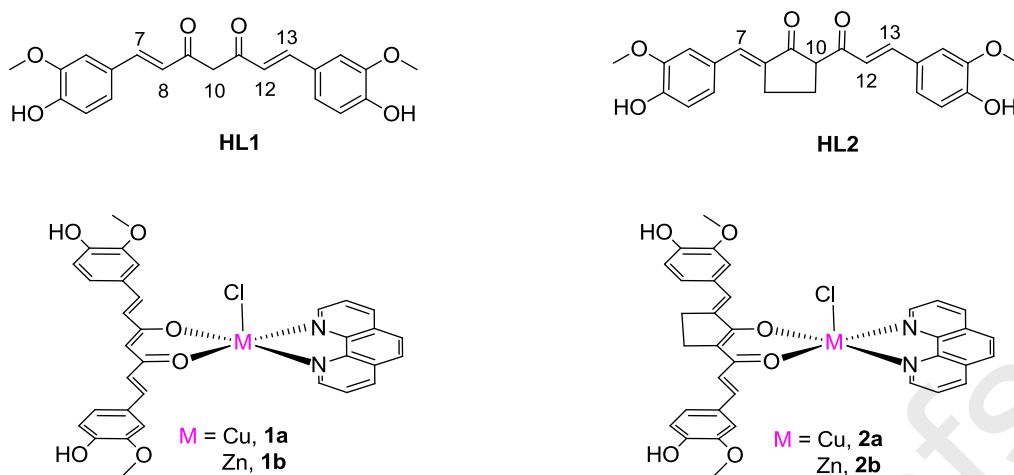


**Figure 1:** Curcuminoid ligands and their Cu(II) and Zn(II) complexes.

The compounds were characterized by spectroscopic techniques, including single crystal X-ray diffraction for **1b**. Finally, their trypanocidal activities were evaluated towards amastigote forms of *T. cruzi*, analyzing the effect of complexation on the activities *in vitro*.

## 2. Experimental

### 2.1. Materials and Methods

All chemicals and solvents were purchased from Sigma-Aldrich, unless otherwise stated, and were used as received. Curcumin (**HL1**) was prepared following a procedure described in the literature [27]. Complex [Zn(**L1**)(phen)Cl] (**1b**) has been reported previously and was synthesized in this work after changing the described methodology [31]. Melting points were measured in a PFM II capillary. IR spectra were recorded in the ATR mode on a FT-IR Bruker Vertex 70 spectrophotometer.  $^1\text{H}$  NMR (500 MHz) spectra were recorded with a Bruker Ultrashield Plus in DMSO- $d_6$ ; chemical shifts are reported in parts per million (ppm) relative to an internal standard of  $\text{Me}_4\text{Si}$ . The hydrogen

signals were assigned based on the coupling constant values and 2D  $^1\text{H} \times ^1\text{H}$  – COSY experiments. 77 K frozen DMSO/H<sub>2</sub>O solution EPR spectra of the Cu(II) complexes were obtained employing a Bruker EMX X-band continuous wave spectrometer configured to 300 ms of conversion time, 40.96 ms of time constant, 600 s of sweep time, 1.0 G of modulation amplitude and 2500 points of spectral resolution. The corresponding spin Hamiltonian simulations were done using the EasySpin software package [35]. Electronic spectra were recorded on a UV-1800 Shimadzu spectrophotometer using MeOH, in five different concentrations in order to calculate the molar absorptivity values ( $\epsilon$ ). Molar conductivities were determined from a  $1.0 \times 10^{-3}$  mol L<sup>-1</sup> solution of the complexes in DMSO, using an ion 120 W microprocessor conductivity meter. Elemental analyses of CHN were performed in a Perkin-Elmer CHN 2400.

## 2.2. Synthesis

### 2.2.1. Synthesis of the curcuminoid ligand **HL2**

2-Acetylcyclopentanone (0.6 mL, 5 mmol), vanillin (1.5 g, 10 mmol) and tributylborate (5.4 mL, 20 mmol) were added into a suspension of boric anhydride (175 mg, 2.5 mmol) in 15 mL of ethyl acetate, forming a yellow solution. The reaction was kept under stirring for 5 min at 50 °C. A solution of 2-aminobutane (0.2 mL, 2.5 mmol) in 2.5 mL of ethyl acetate was added drop wise to the reaction for 15 min until the solution turned from yellow to orange. The temperature was raised to 80 °C and the reaction was stirred for 3 h. Afterwards, 15 mL of aqueous hydrochloric acid (1 mol L<sup>-1</sup>) were added, and the reaction was stirred for an additional 30 min. The resulting orange precipitate was filtered under vacuum and washed with hot ethanol.

(E)-2-(4-hydroxy-3-methoxybenzylidene)-6-((E)-3-(4-hydroxy-3-methoxyphenyl)acryloyl)cyclopentanone, HL2. Yield: 1.2 g, 62 %; m.p. 222-224 °C. HRMS/ESI(m/z): Calculated for [M+H<sup>+</sup>]: (394.1416), found: (394.1416). FTIR (ATR, cm<sup>-1</sup>): 3513 (νOH)<sub>ar</sub>, 3253 (νOH)<sub>enol</sub>, 1623 (νC=O). <sup>1</sup>H NMR (500 Mz, DMSO-d<sub>6</sub>) δ (ppm): 9.66 (s, 1H); 9.63 (s, 1H), 7.50 (d, 1H, *J* = 20 Hz); 7.36 (s, 1H); 7.22 (m, 3H) 7.14 (d, 1H, *J* = 10 Hz); 6.89 (d, 1H, *J* = 10 Hz); 6.84 (d, 1H, *J* = 10 Hz); 6.76 (d, 1H, *J* = 20 Hz); 3.86 (s, 3H); 3.85 (s, 3H); 3.01 (s, 2H); 2.90 (s, 2H). UV-Vis [CH<sub>3</sub>OH; λ/nm (deprotonated)]: 263 (260), (345), 450 (450), (472).

### 2.2.2. Synthesis of Cu(II) and Zn(II) complexes

The curcuminoid ligand (**HL1** or **HL2**) (0.15 mmol) was suspended in CH<sub>3</sub>CN (5 mL), followed by addition of Et<sub>3</sub>N (0.18 mmol) and a solution of phen (0.15 mmol) in 2 mL of CH<sub>3</sub>CN. A solution of the respective metal salt – CuCl<sub>2</sub>·2H<sub>2</sub>O or ZnCl<sub>2</sub> (0.15 mmol) in 3 mL CH<sub>3</sub>CN – was added to the resulting suspension. The reaction was allowed to stir for 5 h at room temperature, and the precipitate was filtrated and washed with CH<sub>3</sub>CN, MeOH and diethyl ether.

[Cu(phen)(L1)Cl].H<sub>2</sub>O, 1a. Yield: 80 %, m.p. 215 °C (decomposition). Elemental analysis of CHN: Calculated for C<sub>33</sub>H<sub>27</sub>ClN<sub>2</sub>O<sub>6</sub>Cu·H<sub>2</sub>O: C, 59.6; H, 4.4; N, 4.2; Found: C, 59.6; H, 4.6; N, 4.1. FTIR (ATR, cm<sup>-1</sup>): 3432 (νOH), 1622 (νC=O), 1589 (νC=N). UV-Vis [CH<sub>3</sub>OH; λ/nm(ε/L mol<sup>-1</sup> cm<sup>-1</sup>): 271 (36,230); 294<sub>sh</sub>; 346; 428 (36,540); 451<sub>sh</sub>.

[Cu(phen)(L2)Cl].H<sub>2</sub>O, 2a. Yield: 74 %, m.p. 212-213 °C (decomposition). Elemental analysis of CHN: Calculated for C<sub>35</sub>H<sub>29</sub>ClN<sub>2</sub>O<sub>6</sub>Cu·H<sub>2</sub>O: C, 60.9; H, 4.5; N, 4.0; Found: C, 61.1; H, 4.6; N, 3.6. FTIR (ATR, cm<sup>-1</sup>): 3369 (νOH), 1620 (νC=O), 1587 (νC=N). UV-Vis [CH<sub>3</sub>OH; λ/nm (ε/L mol<sup>-1</sup> cm<sup>-1</sup>): 270 (24,798); 294<sub>sh</sub>; 357; 456 (20,515); 482<sub>sh</sub>. dd

[Zn(phen)(L1)Cl], **1b**. Yield: 70 %; m.p. 181 °C. Except for X-Ray diffraction analysis, this complex has been previously characterized [31].

[Zn(phen)(L2)Cl]·CH<sub>3</sub>CN·0.8H<sub>2</sub>O, **2b**. Yield: 73 %; m.p. 215-216 °C (decomposition). Elemental analysis of CHN: Calculated for C<sub>35</sub>H<sub>29</sub>ClN<sub>2</sub>O<sub>6</sub>Zn·CH<sub>3</sub>CN·0.8H<sub>2</sub>O: C, 60.9; H, 4.6; N, 5.8; Found: C, 60.5; H, 4.2; N, 5.6. FTIR (ATR, cm<sup>-1</sup>): 3307 (νOH), 1623 (νC=O), 1585 (νC=N). <sup>1</sup>H NMR (500 Mz, DMSO-d<sub>6</sub>): δ (ppm): 9.45 (br m, 2H), 8.89 (br m, 2H), 8.29 (s, 2H), 8.07 (br m, 2H), 7.47-6.65 (m, 9H), 3.83 (s, 6H), 2.89 (m, 4H). UV-Vis [CH<sub>3</sub>OH; λ/nm (ε/L mol<sup>-1</sup> cm<sup>-1</sup>): 266 (20,100); 291<sub>sh</sub>; 348; 450 (77,730); 474<sub>sh</sub>.

### 2.3. Single-crystal X-ray crystallography

Single crystal X-ray data for **1b** were collected on a Bruker D8 Venture diffractometer using graphite-monochromated MoK<sub>α</sub> radiation (λ = 0.71073 Å) at 150 K. Data collection, cell refinement and data reduction were performed with Bruker Instrument Service v4.2.2, APEX2 [36] and SAINT [37], respectively. The absorption correction using equivalent reflections was performed with the SADABS program [38]. The structure solutions and full-matrix least-squares refinements based on  $F^2$  were performed with the SHELXS-97 and SHELXL-2014 programs [39]. All atoms except hydrogen were refined anisotropically. Hydrogen atoms were treated using a constrained refinement. Structure illustrations were generated using the MERCURY program [40]. The title compound weakly diffracts and in the unit cell large voids filled by disordered solvent molecules are present. Although the data were collected at low temperature, the assignment of the intensities related to the solvent molecules failed. Thus, solvent masks routinely implemented on Olex2 program were applied [41]. The total volume of the voids and electrons per unit cell are 2638.2 and 651.4 Å<sup>3</sup>, respectively. The number of

electrons per asymmetric unit corresponds to 81.4 ( $Z=8$ ), which are in good agreement with one acetonitrile and one chloroform molecule as crystallization solvents. A summary of the crystal, data collection and refinement is listed in Table 1.

**Table 1:** Summary of crystal structure, data collection and refinement for **1b**

Compound reference	(1b)
Chemical formula	$C_{33}H_{27}ClN_2O_6Zn$
Formula Mass	648.41
Crystal system	Orthorhombic
$a/\text{\AA}$	22.1942(13)
$b/\text{\AA}$	27.5217(14)
$c/\text{\AA}$	12.6862(8)
Unit cell volume/ $\text{\AA}^3$	7749.0(8)
Temperature/K	120(2)
Space group	Cmc2 <sub>1</sub>
No. of formula units per unit cell, $Z$	8
Radiation type	MoK $\alpha$
Absorption coefficient, $\mu/\text{mm}^{-1}$	0.74
No. of reflections measured	6809
No. of independent reflections	4830
$R_{int}$	0.069
Final $R_I$ values ( $I > 2\sigma(I)$ )	0.056
Final $wR(F^2)$ values ( $I > 2\sigma(I)$ )	0.125
Final $R_I$ values (all data)	0.084
Final $wR(F^2)$ values (all data)	0.136
Goodness of fit on $F^2$	1.04
CCDC Deposition	1945106

#### 2.4. Growth inhibitory activity against *T. cruzi* amastigotes *in vitro*

##### 2.4.1. *In vitro* model for anti-*T. cruzi* assessment

Monkey kidney fibroblasts (LLC-MK2 cells) were seeded in 96-well transparent plates at 10,000 cells/well in 100  $\mu\text{L}$  DMEM medium without phenol red (DMEM-WPR) and with 5% fetal calf serum (FCS). After 12 h incubation for cell adhesion (36  $^\circ\text{C}$ , 5%  $\text{CO}_2$ ), 50,000 trypomastigote forms of *T. cruzi* (Tulahuen C2C4 LacZ strain) were added per well in 20  $\mu\text{L}$  DMEM-WPR + 5% FCS. After 24 h incubation (36  $^\circ\text{C}$ , 5%  $\text{CO}_2$ ), the medium was removed and the wells washed with phosphate buffer saline (PBS,  $2 \times 150$

$\mu\text{L}$ , pre-heated to  $36\text{ }^{\circ}\text{C}$ ). Fresh medium ( $120\text{ }\mu\text{L}/\text{well}$ ) in the presence or absence of the drugs serially diluted from  $100 - 0.41\text{ }\mu\text{M}$  (7 concentrations) was added to the plate prior to further incubation for 120 h ( $36\text{ }^{\circ}\text{C}$ ,  $5\% \text{ CO}_2$ ). The drugs were diluted from a  $100\text{ }\mu\text{M}$  DMEM solution containing  $0.3\%$  DMSO. After inspection under an inverted microscope for assurance of cell development and sterility,  $50\text{ }\mu\text{L}/\text{well}$  of a solution of substrate CPRG ( $0.3\text{ mg}/\text{mL}$ ) and Igepal ( $8\text{ }\mu\text{L}/\text{mL}$ ) was added and the absorbance recorded at  $\lambda = 570\text{ nm}$  after 1 – 2 h incubation ( $36\text{ }^{\circ}\text{C}$ ,  $5\% \text{ CO}_2$ ). The data were converted to a percent cell viability compared to the untreated control and statistically treated using GraphPad Prism 7.00 software. Benznidazole was used as a reference drug.

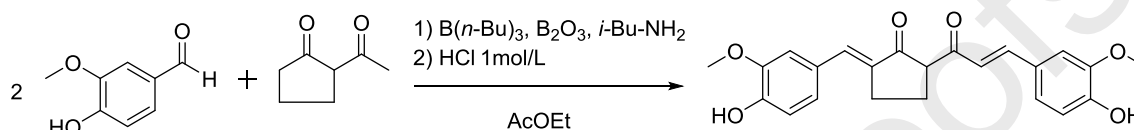
#### 2.4.2 *In vitro* model for LLC-MK2 cytotoxicity assessment

Monkey kidney fibroblasts (LLC-MK2 cells) were seeded in 96-well transparent plates at  $10,000\text{ cells}/\text{well}$  in  $120\text{ }\mu\text{L}$  DMEM-WPR +  $5\%$  FCS. After 24 h incubation ( $36\text{ }^{\circ}\text{C}$ ,  $5\% \text{ CO}_2$ ), the medium was removed and fresh medium ( $120\text{ }\mu\text{L}/\text{well}$ ) in the presence or absence of the drugs serially diluted from  $100 - 0.41\text{ }\mu\text{M}$  (7 concentrations) was added to the plate, which was then incubated for 120 h ( $36\text{ }^{\circ}\text{C}$ ,  $5\% \text{ CO}_2$ ). The drugs were diluted from a  $100\text{ }\mu\text{M}$  DMEM solution containing  $0.3\%$  DMSO. After inspection under an inverted microscope for assurance of cell development and sterility,  $20\text{ }\mu\text{L}/\text{well}$  of a solution of 3-(4,5-dimethyl-2-thiazolyl)-2,5-diphenyl-2H-tetrazolium bromide (MTT salt,  $1.25\text{ mg}/\text{mL}$ ) and 5-methylphenazinium methyl sulfate (PMS,  $0.11\text{ mg}/\text{mL}$ ) was added, following 2 – 3 h of incubation ( $36\text{ }^{\circ}\text{C}$ ,  $5\% \text{ CO}_2$ ). After medium removal, MTT formazan crystals were solubilized in  $100\text{ }\mu\text{L}$  DMSO and the absorbance recorded at  $\lambda = 570\text{ nm}$ . The data were converted to a percent cell viability and compared to the untreated control and statistically treated using GraphPad Prism 7.00 software. Triton X ( $0.1\% \text{ v}/\text{v}$ ) was used as positive control.

### 3. Results and Discussion

#### 3.1. Synthesis of the ligand **HL2**

The curcuminoid ligand **HL2** was obtained by reacting vanillin and acetylcyclopentanone in the presence of tributylborate, boric anhydride and 2-aminobutane (Scheme 1).

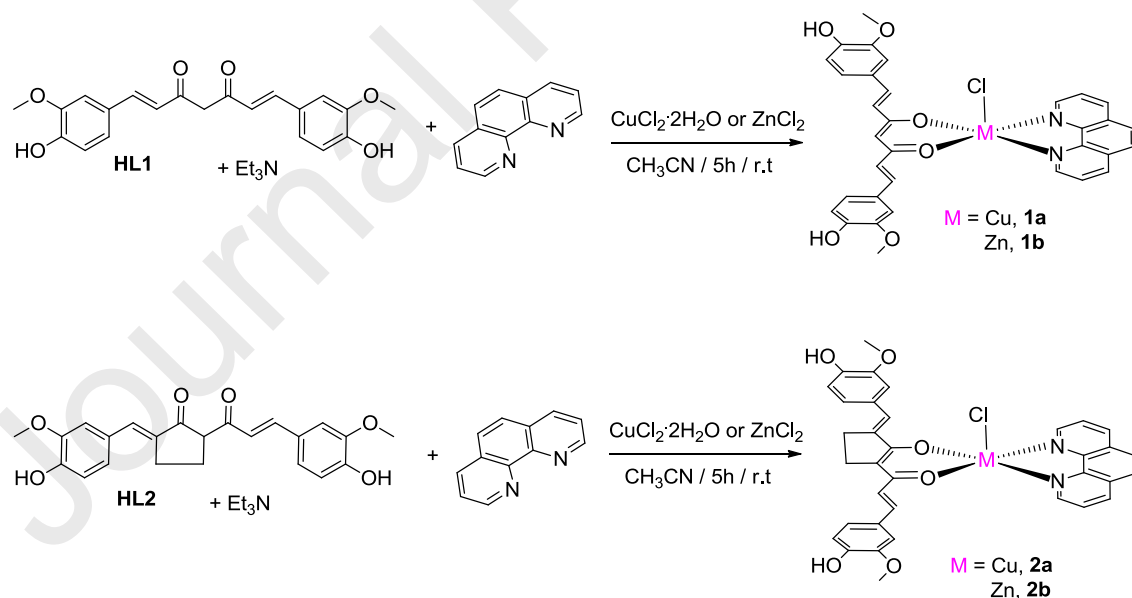


**Scheme 1:** Synthesis of **HL2**.

These conditions are classical for the Pabon synthesis, which gives yields higher than those previously described in literature [42]. Boric anhydride and tributylborate were used to form a boron-based enolate with the 1,3-dicarbonyl compound, so the nucleophilic addition to the aldehyde carbonyl is selective for the appropriate carbons, since the more acidic proton is the one between the carbonyls. After formation of the complex, the amine reacted with the remaining acidic protons and the condensation with the aldehyde occurred in the boron-based enolate itself, which was subsequently disrupted by the addition of the acid solution to generate a yellow precipitate, which was isolated by filtration. Washing the precipitate with hot ethanol removed both impurities and byproducts formed. The **HL2** carbocyclic derivative was purified by recrystallization from a hydroalcoholic mixture and suitably characterized by MS, FTIR and NMR, and subsequently used for the complexation reactions.

## 3.2. Synthesis of the Cu(II) and Zn(II) complexes

The complexes were obtained by mixing a suspension of the curcuminoid ligand in acetonitrile containing Et<sub>3</sub>N and the auxiliary ligand (phen), followed by the addition of the metal salt (CuCl<sub>2</sub>·2H<sub>2</sub>O or ZnCl<sub>2</sub>), also in CH<sub>3</sub>CN (Scheme 2). Et<sub>3</sub>N was used with the aim to deprotonate the curcuminoid. After 5 h, the precipitate was extensively washed with acetonitrile and methanol to remove unreacted precursors. Complex [Zn(phen)(L1)Cl] (**1b**) has been reported previously in the literature [31] and was successfully synthesized in this work. IR (SI, Fig. S4), UV-Vis (SI, Fig. S8), <sup>1</sup>H NMR (SI, Fig. S10) and melting point (181 °C) analyses agreed well with those described in the reference [31]. Additionally, single crystals of **1b** suitable for X-ray diffraction analysis were obtained by slow evaporation of a solution of a 1:1 solution of the complex in CH<sub>3</sub>CN/CHCl<sub>3</sub>. This structure has not yet been reported in the literature.



**Scheme 2:** Synthesis of the complexes [M(L1-2)(phen)Cl] (M = Cu(II) or Zn(II)), containing curcuminoid and phen ligands. The Zn(II) complex (**1b**) was previously reported [31].

### 3.3. General characterization

The IR spectra of **HL1-2** (SI, Fig. S1-S2) showed a sharp band around  $3500\text{ cm}^{-1}$  associated with the OH from the aromatic rings [27]. In addition, a broad band was observed at about  $3200\text{ cm}^{-1}$ , due to the OH from the enolic form of the ligands [27]. For **1a-b**, **2a-b** (SI, Figs. S3-S6), the OH frequencies were detected in the range of  $3300\text{-}3200\text{ cm}^{-1}$ . All complexes exhibited absorption in the region of  $1620\text{ cm}^{-1}$  associated with stretching vibrations of  $\nu\text{C=O}$ . These signals were not significantly shifted compared to the ligands [27] and could be explained by the intermediate character between a double and a single C–O bond, both in the enolic form of the ligand and in the complex. **1a-b**, **2a-b** also displayed a new absorption around  $1585\text{ cm}^{-1}$  attributed to  $\nu\text{C=N}$  [31] indicating coordination with phen. Finally, a sharp signal within  $1500\text{-}1510\text{ cm}^{-1}$  was associated to the C–C–C chelated ring [31] and appeared in the spectra of all compounds.

The  $^1\text{H}$  NMR spectra of the free ligands (**HL1** and **HL2**) displayed singlets at  $\delta$  9.71 (for **HL1**) and  $\delta$  9.66 and 9.63 (for **HL2**) attributed to phenolic OH, which are absent in the spectra of the corresponding complexes  $[\text{Zn}(\text{L1-2})(\text{phen})\text{Cl}]$  **1b** [31] and **2b** (SI, Fig. S9-10). Both ligands are in the enolic form in solution, confirmed by the lack of the signal corresponding to C–H10 in the spectra (SI, Fig. S9-10). The aromatic C–H and  $\text{C}_{\text{sp}2}\text{-H}$  peaks were found in the expected region ( $\sim \delta$  7.5-6.5) for the ligands, with small shifts upon coordination. Finally, the presence of coordinated phen was confirmed by the characteristic signals around  $\delta$  9.50, 8.90, 8.30 and 8.10 for **1b** and **2b**.

The electronic spectra of the complexes, recorded in MeOH (SI, Fig. S7-S8), showed typical  $\pi\text{-}\pi^*$  transitions of the extended conjugation system from the curcuminoid ligand [27], between 426 and 453 nm with a shoulder around 448-478 nm. The intense absorption observed at 270 nm with a shoulder at 290 nm was associated with the ligands (curcuminoid and phen) [43].

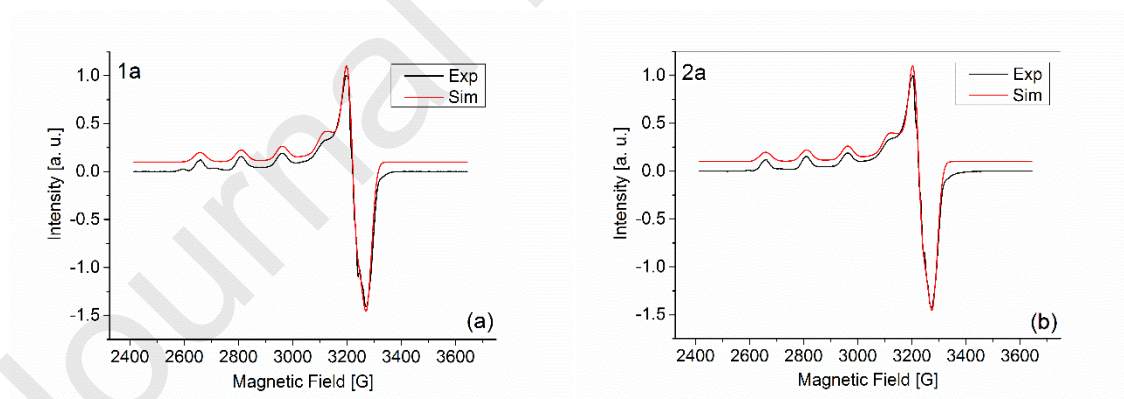
To further investigate the complexes in solution, conductivity data were determined in DMSO. The results are compiled in Table 2.

Table 2: Conductivity data ( $\mu\text{S cm}^{-1}$ ) of complexes **1a–b**, **2a–b** in DMSO at  $1.0 \times 10^{-3} \text{ mol L}^{-1}$ .

Compound	Time	
	0 h	24 h
<b>1a</b>	11	12
<b>1b</b>	12.	16
<b>2a</b>	12.	11
<b>2b</b>	12	15

The conductivity values indicate that the complexes behave as non-electrolytes [44] and confirm their solution stability within 24 h.

The copper complexes were studied by electron paramagnetic resonance (EPR) and the spectra from the frozen DMSO/H<sub>2</sub>O 1:1 solution of both **1a** and **2a** along with simulations are presented in Figure 2.



**Figure 2:** 77 K frozen DMSO/H<sub>2</sub>O 1:1 solution spectra of complexes **1a** (a) and **2a** (b).

The black line is the experimental spectrum (Exp), the red line the simulated spectrum (Sim).

Employing the approach devised by Peisach and Blumberg [45] it is demonstrated that the spectra from both complexes comprise one major component derived from a distinct static Jahn-Teller elongated configuration, with the orbital  $3d_{x^2-y^2}$  being the lowest in energy. This static configuration renders both  $g$  and  $A$  tensors axial, which is confirmed by the spin Hamiltonian parameters obtained from the simulations, presented in Table 3.

**Table 3:** EPR spectra simulation parameters for **1a** and **2a**.

Complex	$g_{\parallel}$	$g_{\perp}$	$A_{\parallel}$ [MHz]	$A_{\perp}$ [MHz]
<b>1a</b>	2.3142	2.0712	480.32	< 50
<b>2a</b>	2.3145	2.0684	481.03	< 50

The concerned conformation emerges when the static Jahn-Teller axis is set perpendicular to the plane formed by the two ligands, which corresponds to an equatorial coordination ring comprising two oxygen atoms from the curcuminoid moiety and two nitrogen atoms from the phen moiety (2N2O). This attribution is validated by comparing the parameters of the spin Hamiltonian simulations to the values on the  $g_{\parallel}/A_{\parallel}$  diagrams on [45].

The results of the EPR studies agreed to the proposed crystallographic structure for the analyzed complexes.

### 3.4. Crystal structure of **1b**

Single crystals were obtained by slow evaporation of a  $\text{CH}_3\text{CH}/\text{CHCl}_3$  1:1 solution containing **1b**. The compound crystallized in the chiral orthorhombic  $Cmc2_1$  space group, displaying two crystallographic independent molecules in the asymmetric unit, as shown

separately in Figure. 3. For the sake of comparison, from now on the molecules will be labelled as A and B. Selected bond lengths and angles are listed in Table 4.

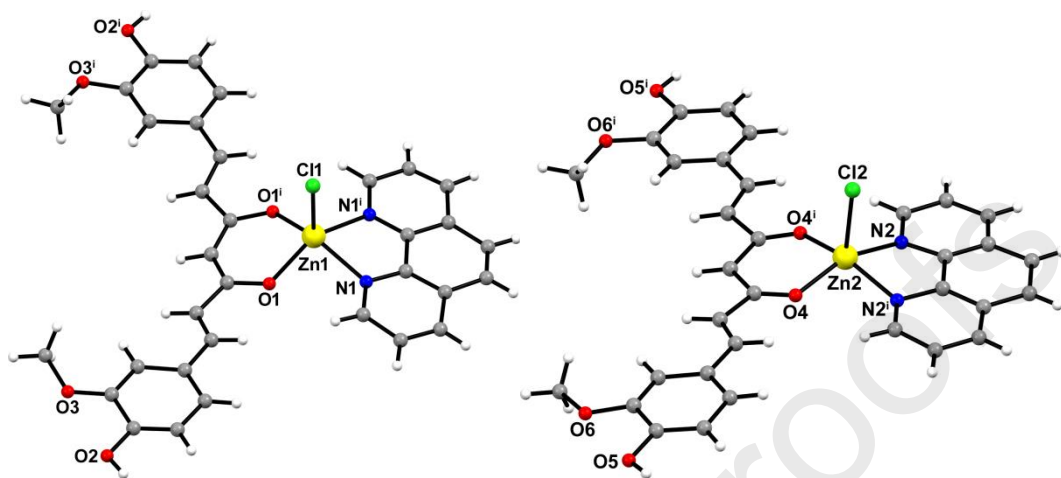


**Figure 3:** Crystal structures of the independent molecules in the asymmetric unit of compound **1b** (molecule A: left, molecule B: right).

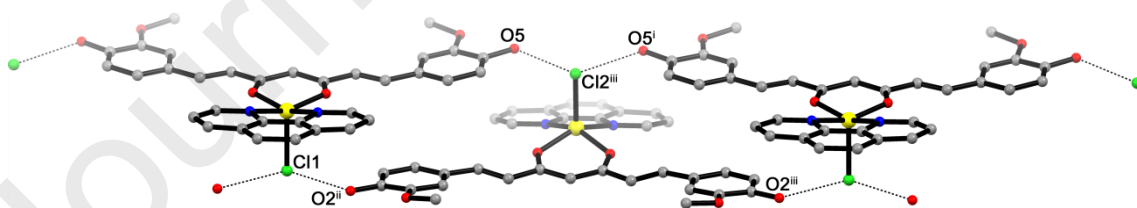
**Table 4.** Selected bond lengths (Å) and angles (°) for compound **1b** ( $i = -x, y, z$ )

Atom labels	<b>1b</b>
Zn1—Cl1	2.280(3)
Zn1—O1	2.010(5)
Zn1—N1	2.157(5)
Zn2—Cl2	2.408(5)
Zn2—O4	1.992(5)
Zn2—N2	2.280(3)
O1—C2	1.307(9)
C1—C2	1.354(9)
O4—C13	1.200(8)
C12—C13	1.462(9)
N1—Zn1—Cl1	103.5(2)
O1—Zn1—Cl1	106.41(2)
N1—Zn1—O1	88.4(2)
O1—Zn1—O1 <sup>i</sup>	91.2(3)
O1 <sup>i</sup> —Zn1—N1 <sup>i</sup>	88.4(2)
N1—Zn1—N1 <sup>i</sup>	76.5(3)
Cl1—Zn1—O1 <sup>i</sup>	106.4(2)
Cl1—Zn1—N1 <sup>i</sup>	103.5(2)
N1—Zn1—O1 <sup>i</sup>	148.9(3)
N2—Zn2—O4	157.8(3)
N2—Zn2—Cl2	98.9(2)
O4—Zn2—Cl2	102.1(2)
N2—Zn2—N2 <sup>i</sup>	80.1(3)
N2—Zn2—O4 <sup>i</sup>	89.7(2)
O4—Zn2—N2 <sup>i</sup>	89.7(2)
O4—Zn2—O4 <sup>i</sup>	92.8(3)
Cl2—Zn2—N2 <sup>i</sup>	98.9(2)
Cl2—Zn2—O4 <sup>i</sup>	102.1(2)

In both molecules the metal ion is pentacoordinated to one deprotonated curcumin and one phenanthroline molecules in the basal plane, while the axial position is filled by one chlorido ligand. The coordination geometry of the zinc(II) ions is closer to a trigonal bipyramid, confirmed by the Addison's trigonality parameter [46],  $\tau$ , for both molecules:

0.92 and 0.76 for A and B, respectively. Although they presented a similar coordination environment, the geometry around the zinc ion in molecule B is slightly more distorted from ideality than in A. The bond lengths Zn–Cl and Zn–O<sub>curcumin</sub> and Zn–N<sub>phen</sub> are typical for other similar compounds reported elsewhere [47]. It is important to highlight that the curcumin moiety is planar, suggesting its coordination is in the diketonate form due to electronic delocalization. However, differences could also be observed in the curcumin coordination when A and B are compared. In molecule B, the metal ion is contained in the curcumin plane, while in A, the zinc(II) ion is displaced by ca. 2 Å from it, as a consequence of the more pronounced trigonal bipyramidal geometry.

The crystal packing is stabilized by a network of hydrogen bonds involving the curcumin hydroxyl group and the chlorido ligands from A and B, leading to a supramolecular chain running along the [1 0 0] direction, as seen in Figure 4a. The distances between the acceptor and donor atoms are 3.096(11) for C11...O2<sup>ii</sup>, and 3.138(10) for C12<sup>iii</sup>...O5 (ii = -1/2+x, 3/2-y, -1/2+z and iii = -1/2-x, 3/2-y, -1/2+z). Moreover, in the bc plane, the layers of molecules A (pink) and B (blue) are positioned in an alternating way (Figure 4b).



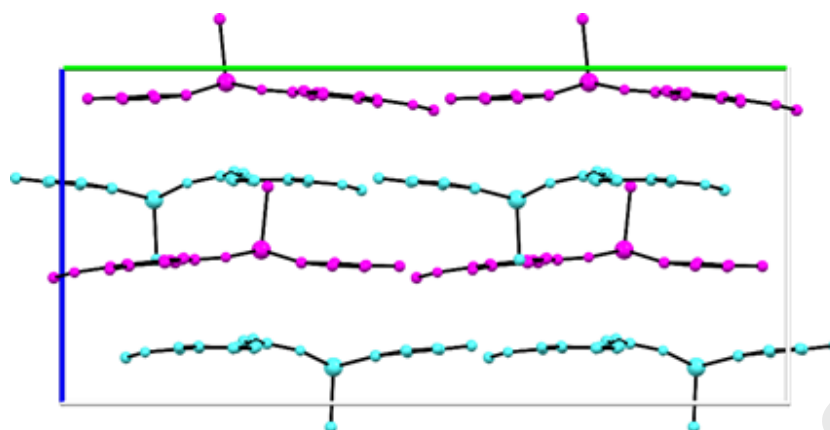


**Figure 4:** Details of the crystal packing of compound **1b**: (a) intermolecular interactions involving chlorido and curcumin hydroxyl groups (above). Symmetry operations to generate equivalent atoms: i = -x, y, z; ii = -1/2+x, 3/2-y, -1/2+z; iii = -1/2-x, 3/2-y, -1/2+z. (b) Layers of molecules A and B in the crystallographic bc plane (bottom). Hydrogen atoms were omitted for the sake of clarity.

### 3.5. *In vitro* activity assessment against amastigotes of *T. cruzi* and cell line LLC-MK2

The trypanocidal activity of the compounds has been evaluated *in vitro* using the Tulahuen-C2C4 LacZ strain in the amastigote form internalized in the mammalian cell line LLC-MK2 (rhesus monkey kidney fibroblasts). The inhibitory concentrations of cell proliferation at 50% (IC<sub>50</sub>) are presented in Table 5, expressed as the average of three independent experiments and the standard deviation ( $\sigma$ ).

**Table 5:** IC<sub>50</sub> values against *T. cruzi* and LLC-MK2 cells.

Compound	<i>T. cruzi</i> IC <sub>50</sub> ± $\sigma$ ( $\mu$ M)	LLC-MK2 IC <sub>50</sub> ± $\sigma$ ( $\mu$ M)	SI <sup>a</sup>
<b>HL1</b>	9.35 ± 1.31	12.54 ± 1.78	1.3 <sup>ns</sup>
<b>HL2</b>	1.99 ± 0.61	6.15 ± 0.35	3.1 <sup>**</sup>
<b>1a</b>	2.30 ± 0.10	2.74 ± 0.29	1.2 <sup>ns</sup>
<b>1b</b>	0.47 ± 0.12	2.02 ± 0.51	4.3 <sup>**</sup>
<b>2a</b>	1.65 ± 0.20	2.73 ± 0.13	1.7 <sup>*</sup>
<b>2b</b>	0.40 ± 0.12	1.52 ± 0.28	3.8 <sup>**</sup>
<b>Phen</b>	0.94 ± 0.20	2.92 ± 0.63	3.1 <sup>*</sup>

<b>CuCl<sub>2</sub>·2H<sub>2</sub>O</b>	> 100	> 100	-
<b>ZnCl<sub>2</sub></b>	> 100	> 100	-
<b>Benznidazole</b>	1.45 ± 0.20	> 100	> 70

SI = selectivity index =  $(IC_{50}^{T. cruzi})/(IC_{50}^{LLC-MK2})$ ; a P value from Welch's t test: ns = P > 0.05 (not significant), \* = P < 0.05, \*\* P < 0.01

The ligands and complexes generally displayed high toxicity against both host cell LLC-MK2 and *T. cruzi*. This result was expected. Curcuminoid compounds have had their anti-proliferative profiles previously described against tumor cell lines [48-50] as well as trypanosomatids [16,51,52]. Our findings also demonstrated that metal complexation improved the biological activity of both curcuminoid ligands, as initially intended.

Comparatively, the zinc complexes **1b** ( $IC_{50} = 0.47 \mu\text{M}$ , SI = 4.3) and **2b** ( $IC_{50} = 0.47 \mu\text{M}$ , SI = 4.3) were more toxic towards the parasite and more selective than the ligands (**HL1**, **HL2**, **phen**) as well as the copper complexes (**1a**, **2a**), implying that the complexing metal is important to the mode of action of these compounds.

The varying selectivity profiles of the compounds are depicted in Figure 5. The graphs show the average cell viability vs concentration, with error bars representing the standard deviation. One can observe a higher superposition for the graphs representing the compounds with the lowest SI (**HL1**, **1a**, **2a**). Zinc complexes (**1b**, **2b**) on the other hand, besides showing a higher selectivity for the parasite, were able to eradicate *T. cruzi* in concentrations as low as  $1.3 \mu\text{M}$ , while preserving around 50-60% of host cells. Even though the Zn(II) complexes have been more potent than the benznidazole, they were not as selective as the reference drug.

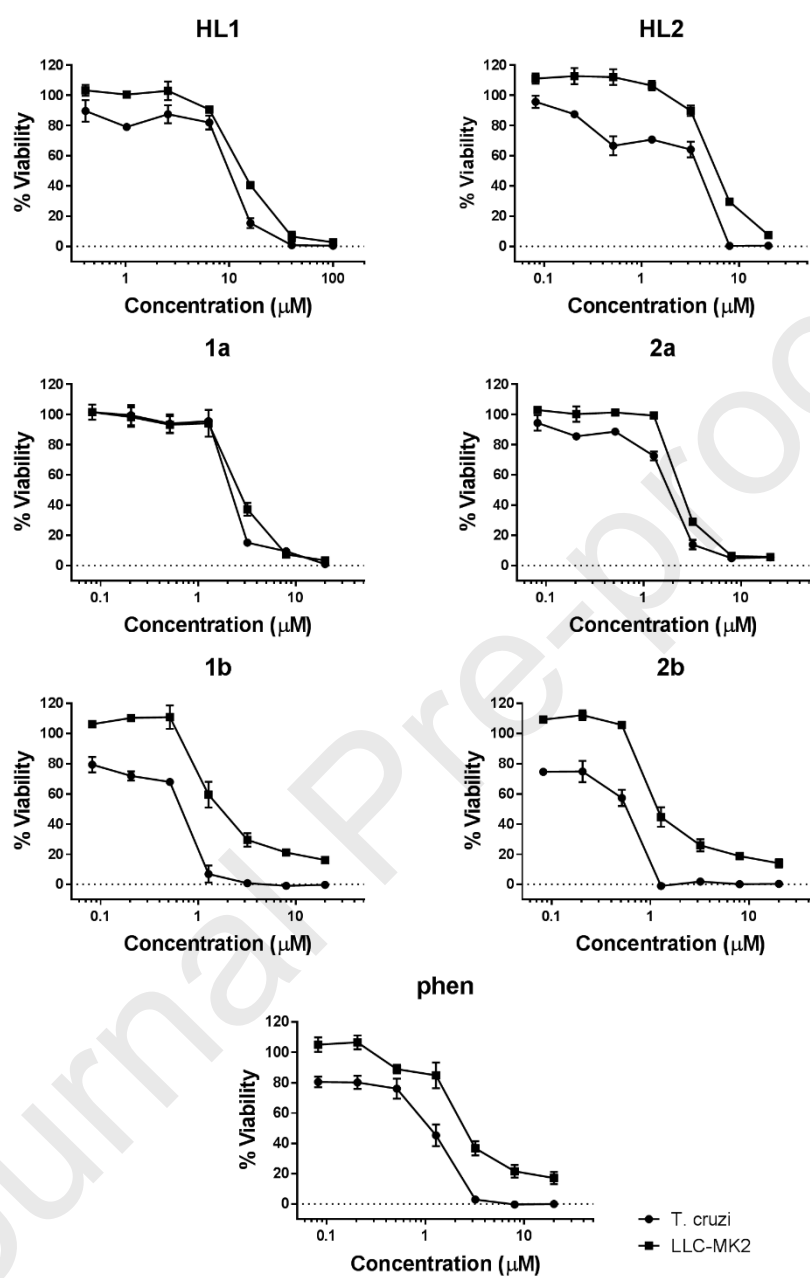


Figure 5: Comparative *in vitro* cytotoxicity against *T. cruzi* and LLC-MK2 cells.

#### 4. Conclusions

A series of Cu(II) and Zn(II) complexes containing curcuminoids and phen ligands were obtained and characterized. The crystal structure determined for [Zn(L1)(phen)Cl] (**1b**) confirmed the structure previously proposed in the literature. The curcuminoid (L) coordinates in the anionic form through the  $\beta$ -diketonate group in a 1:1 ligand:metal proportion and phen is bound through the nitrogen atoms with a chlorido ligand completing the coordination sphere of the metal. NMR and EPR spectroscopy evidenced that the other complexes exhibited the same structure of **1b**. Anti-parasitic investigation against *T. Cruzi* revealed that the Zn(II) complexes were the most potent compounds against the parasite, and also exhibited the best selectivities - except when compared to benznidazole. Finally, complexation of the curcuminoid ligands lead to an enhancement of trypanocidal activities, besides the presence of phenanthroline that also contributed to the great toxicity exhibited by the complexes.

#### Acknowledgements

The authors thank LDRX-UFF ([www.ldrx.uff.br/](http://www.ldrx.uff.br/)) for the X-ray diffraction analysis and PPGQ-UFRRJ (<http://cursos.ufrrj.br/posgraduacao/ppgq/>) for the facilities. This study was financed in part by the Coordenação de Aperfeiçoamento de Pessoal de Nível Superior - Brasil (CAPES) - Finance Code 001, CNPq (BR) and FAPERJ (BR) (grant: E26/200.991/2014).

## Appendix A. Supplementary data

Supporting information to this article contains additional data for the spectroscopic characterization of the compounds. X-ray crystallographic data in cif format available at CCDC 1945106 can be obtained free of charge via [www.ccdc.cam.ac.uk/data\\_request/cif](http://www.ccdc.cam.ac.uk/data_request/cif).

## References

- [1] S. Antinori, L. Galimberti, R. Bianco, R. Grande, M. Galli, M. Corbellino, *Eur. J. Intern. Med.* 43 (2017) 6-15.
- [2] L. Stevens, P. L. Dorn, J. O. Schmidt, J. H. Klotz, D. Lucero, S. A. Klotz, *Adv. Parasitol.* 75 (2011) 169-192.
- [3] [http://www.who.int/en/news-room/fact-sheets/detail/chagas-disease-\(american-trypanosomiasis\)](http://www.who.int/en/news-room/fact-sheets/detail/chagas-disease-(american-trypanosomiasis)), accessed in April 2019.
- [4] F. R. Matins-Melo, M. Carneiro, A. L. P. Ribeiro, J. M. T. Bezerra, G. L. Werneck, *Int. J. Parasitol.* 49 (2019) 301–310.
- [5] J. A. Pérez-Molina, I. Molina, *Lancet.* 391 (2018) 82-94.
- [6] J. Clayton, *Nature.* 465 (2010) S4-S5.
- [7] V. Sueth-Santiago, D. Decote-Ricardo, A. Morrot, C. G. Freire-de-Lima, M. E. F. Lima, *World J. Biol. Chem.* 8 (2017) 57-80.
- [8] V. G. Duschak, *Curr. Drug Targets.* 20 (2019) 1203-1216.
- [9] P. Gupta, S. Khan†, M. M. Manzoor, A. K. Yadav, G. Sharma, R. Anand, S. Gupta, *Stud. Nat. Prod. Chem.* 54 (2017) 355-401.
- [10] A. Amalraj, A. Pius, S. Gopi, S. Gopi, *J. Tradit. Complement. Med.* 7 (2016) 205-233.

- [11] J. Wickenberg, S. L. Ingemansson, J. Hlebowicz, *Nutrition Journal*. 9 (2010) 1-5.
- [12] A. Siviero, E. Gallo, V. Maggini, L. Gori, A. Mugelli, F. Firenzuoli, A. Vannacci, J. *Herb. Med.* 5 (2015) 57-70.
- [13] N. Boroumand, S. Samarghandian, S. I. Hashemy, J. *Herbmed Pharmacol.* 7 (2018) 211-219.
- [14] D. Mathew, W.-L. Hsu, *J. Func. Foods.* 40 (2018) 692-699.
- [15] L. M. Souza, N. M. Inada, F. P. Venturini, C. C. Carmona-Vargas, S. P. Vieira, K. T. Oliveira, C. Kurachi, V. S. Bagnato, *J. Asia Pac. Entomol.* 22 (2019) 151–158.
- [16] V. Sueth-Santiago, J. B. B. M. Alves, E. S. S. M. A. Vannier-Santos, C. G. Freire-de-Lima, R. N. Castro, G. P. Mendes-Silva, C. N. Del Cistia, L. G. Magalhães, A. D. Andricopulo, C. M. R. Sant`anna, D. Decotè-Ricardo, M. E. F. Lima, *Plos One*. 11 (2016) 1-20.
- [17] D. Sun, X. Zhuang, X. Xiang, Y. Liu, S. Zhang, C. Liu, S. Barnes, W. Grizzle, D. Miller, H. G. Zhang, *Mol. Ther.* 18 (2010) 1606–1614.
- [18] P. Anand, A. B. Kunnumakkara, R. A. Newman, B. B. Aggarwal, *Mol. Pharmaceutics*. 4 (2017) 807-818.
- [19] S. S. Bansal, M. Goel, F. Aqil, M. V. Vadhanam, R. C. Gupta, *Cancer Prev. Res.* 4 (2011) 1158 –1171.
- [20] D. Pucci, R. Bloise, A. Bellusci, S. Bernardini, M. Ghedini, S. Pirillo and A. Valentini, *J. Inorg. Biochem.* 101 (2007) 1013-1022.
- [21] A. Valentini, F. Conforti, A. Crispini, A. De Martino, R. Condello, C. Stellitano, G. Rotilio, M. Ghedini, G. Federici, S. Bernardini, D. Pucci. *J. Med. Chem.* 52 (2009) 484-491.

- [22] F. Caruso, M. Rossi, A. Benson, C. Opazo, D. Freedman, E. Monti, M. B. Gariboldi, J. Shaulky, F. Marchetti, R. Pettinari, C. Pettinari, *J. Med. Chem.* 55 (2012) 1072-1081.
- [23] J. R. Lou, X.-X. Zhang, J. Zheng, W.-Q. Ding, *Anti-cancer Res.* 30 (2010) 3249-3255.
- [24] N. Saewan, A. Thakam, A. Jintaisong, K. Kittigowitana, *Int. J. Pharm. Pharm. Sci.* 6 (2014) 270-273.
- [25] B. Banik, K. Somyajit, G. Nagaraju, A. R. Chakravarty, *Dalton Trans.* 43 (2014) 13358-13369.
- [26] K. K. Sharma, S. Chandra, D. K. Basu, *Inorg. Chim. Acta.* 135 (1987) 47-48.
- [27] M. A. Subhan, K. Alam, M. S. Rahaman, M. A. Rahaman, M. R. Awal, *J. Sci. Res.* 6 (2014) 97-109.
- [28] M. Prohl, U. S. Schubert, W. Weigand, M. Gottschaldt, *Coord. Chem. Rev.* 41 (2016) 32-41.
- [29] I. Ali, K. Saleem, D. Wesselinova, A. Haque, *Med. Chem. Res.* 22 (2013) 1386-139.
- [30] S. Banerjee, P. Prasad, A. Hussain, I. Khan, P. Kondaiah, A. R. Chakravarty, *Chem. Commun.* 48 (2012) 7702-7704.
- [31] D. Pucci, A. Crispini, B. S. Mendiguchía, S. Pirillo, M. Ghedini, S. Morelli, L. Bartolo, *Dalton Trans.* 42 (2013) 9679-9687.
- [32] B. S. Mendiguchia, I. Aiello, A. Crispini, *Dalton Trans.* 44 (2015) 9321-9334.
- [33] A. Tarushi, G. PSomas, C. P. Raptopoulou, D. P. Kessissoglou, *J. Inorg. Biochem.* 103 (2009) 898-905.

- [34] E. K. Efthimiadou, N. Katsaros, A. Karaliota, G. Psomas, J. Inorg. Chim. Acta. 360 (2007) 4093-4102.
- [35] S. Stoll, A. Schweiger, J. Magn. Reson. 178 (2006) 42-55.
- [36] Bruker APEX2 v2014.5-0, Bruker AXS Inc., Madison, Wisconsin, USA (2007).
- [37] SAINT V8.34A, Bruker AXS Inc., Madison, Wisconsin, USA (2013).
- [38] G. M. Sheldrick, SADABS: Program for Empirical Absorption Correction of Area Detector Data. University of Göttingen, Germany (1996).
- [39] G. M. Sheldrick, Acta Crystallogr. C Struct. Chem. 71 (2015) 3-8.
- [40] C. F. Macrae, P. R. Edgington, P. McCabe, E. Pidcock, G. P. Shields, R. Taylor, M. Towler, J. Van de Streek, J. Appl. Cryst. 39 (2006) 453-457.
- [41] O. V. Dolomanov, L. J. Bourhis, R. J. Gildea, J. A. K. Howard, H. Puschmann, J. Appl. Cryst. 42 (2009) 339-341.
- [42] H. J. J. Pabon, Recueil des Travaux Chimiques des Pays-Bas. 83 (2010) 379-386.
- [43] N. Armoroli, L. Cola, V. Balzani, J. P. Sauvage, C. O. Dietrich-Buchecker, J. M. Kern, J. Chem. Soc. Faraday Trans. 88 (1992) 553-556.
- [44] W. J. Geary, Coord. Chem. Rev. 7 (1971) 81-122.
- [45] J. Peisach, W. E. Blumberg, Arch. Biochem. Biophys. 165 (1974) 691-708.
- [46] A. W. Addison, T. N. Rao, J. van Reedijk, J. V. Rijn, G. C. Verschoor, J. Chem. Soc., Dalton Trans. 7 (1984) 1349-1356.
- [47] L.-J. Yang, Q.-L. Liu, M.-X. Wang, L.-S. Gu, Y.-H. Luo, B.-W. Sun, Spectrochim. Acta A. Mol. Biomol. Spectrosc. 166 (2016) 1-7.

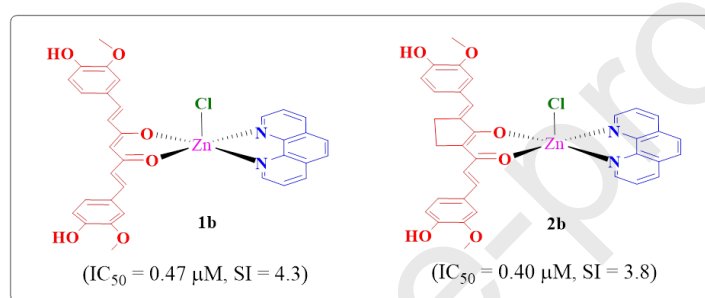
- [48] J. Shi, X. Zhang, T. Shi, H. Li, *Oncol. Lett.* 14 (2017) 1157-1161.
- [49] J. H. Hong, K. S. Ahn, E. Bae, S. S. Jeon, H. Y. Choi, *Prostate Cancer Prostatic Dis.* 9 (2006) 147-152.
- [50] T. M. Elattar, A. S. Virji, *Anticancer Res.* 20 (2000) 1733-1738.
- [51] D. C. Gomes, L. V. Alegrio, M. E. Lima, L. L. Leon, C. A. Araújo, *Arzneimittelforschung.* 52 (2002) 120-124.
- [52] F. Nagajyothi, D. Zhao, L. M. Weiss, H. B. Tanowitz, *Parasitol. Res.* 110 (2012) 2491-2499.

**Highlights**

- Four Cu(II) and Zn(II) complexes with curcuminoid-based ligands (L1-2) have been synthesized
- Complexes are neutral with general formula  $[M(L1-2)(phen)Cl]$ , M = Cu(II) or Zn(II)
- Ligands and complexes have shown significant toxicity against amastigote form of *T. cruzi*
- The Zn(II) compounds were the most potent and selective towards the parasite

## Graphical Abstract

A series of curcuminoid metal complexes of the type  $[M(L1-2)(phen)Cl]$  **1a-b**, **2a-b**, where  $M = Cu(II)$  or  $Zn(II)$  were investigated against amastigote form of *T. Cruzi* and the  $Zn(II)$  complexes exhibited better activities and selectivity indexes ( $IC_{50}$  **1b** = 0.47  $\mu M$ ,  $SI = 4.3$  and  $IC_{50}$  **2b** = 0.40  $\mu M$ ,  $SI = 3.8$ ) compared to the free ligands and  $Cu(II)$  complexes. As well as the curcuminoid ligand, the presence of phenantroline contributed to the trypanocidal activity of the complexes.



( $IC_{50}$  Benznidazole = 1.45  $\mu M$ ,  $SI > 70$ )

Trypanocidal  
Activity

**Declaration of interests**

The authors declare that they have no known competing financial interests or personal relationships that could have appeared to influence the work reported in this paper.

The authors declare the following financial interests/personal relationships which may be considered as potential competing interests:

Journal Pre-proofs